Clinical Biomechanics 82 (2021) 105284

Contents lists available at ScienceDirect

Clinical Biomechanics

journal homepage: www.elsevier.com/locate/clinbiomech

How does transtrochanteric anterior rotational osteotomy change the dynamic three-dimensional intact ratio in hips with osteonecrosis of the femoral head?

Daisuke Hara [a,b,c,*], Satoshi Hamai [b], Kyle R. Miller [a], Goro Motomura [b], Kensei Yoshimoto [b], Keisuke Komiyama [b], Kyohei Shiomoto [b], Satoshi Ikemura [b], Yasuharu Nakashima [b], Scott A. Banks [a]

[a] Department of Mechanical and Aerospace Engineering, University of Florida, 330 MAE-A, P.O. Box 116250, Gainesville, FL 32611-6250, USA
[b] Department of Orthopaedic Surgery, Graduate School of Medical Sciences, Kyushu University, 3-1-1 Maidashi, Higashi-ku, Fukuoka 812-8582, Japan
[c] Department of Orthopaedic Surgery, Kyushu Rosai Hospital, 1-1 Sonekitamachi, Kokuraminami-ku, Kitakyushu, Fukuoka 800-0296, Japan

ARTICLE INFO

Keywords:
Transtrochanteric rotational osteotomy
Anterior rotational osteotomy
Osteonecrosis of the femoral head
Intact ratio
Hip kinematics
Deep hip flexion

ABSTRACT

Background: The intact ratio (the ratio of the intact area of the femoral head) on a two-dimensional anteroposterior radiograph is associated with the prognosis of hips with osteonecrosis of the femoral head after transtrochanteric anterior rotational osteotomy. However, changes of the three-dimensional intact ratio during dynamic weight-bearing activity and correlation of the three-dimensional intact ratio with clinical scores are still unknown.

Methods: Kinematics of eight hips with osteonecrosis of the femoral head that underwent anterior rotational osteotomy were analyzed using image-matching techniques during chair-rising and squatting preoperatively and postoperatively. Two types of dynamic three-dimensional intact ratios were examined, including the lunate covered area (IR_{LC}) and *in vivo* peak contact force vector intersected area (IR_{FV}). The static three-dimensional intact ratio in each octant of the femoral head was also examined.

Findings: The mean Harris hip score significantly improved from 67 preoperatively to 90 postoperatively. During chair-rising rising/squatting, the mean IR_{LC} and IR_{FV} significantly increased from 42%/41% and 7%/4% preoperatively, to 66%/65% and 79%/77% postoperatively, respectively. IR_{LC} significantly changed during the motion whereas substantial postoperative IR_{FV} was maintained throughout the motion. Additionally, Harris hip score and the static three-dimensional intact ratio in the superolateral regions had significant positive correlations with both IR_{LC} and IR_{FV}.

Interpretation: Hip kinematics affected IR_{LC} but not IR_{FV}, which suggests that substantial intact bone occupies the region in which peak contact forces are applied during deep hip flexion. Additionally, improving intact ratio in the superolateral region led to improvements in both IR_{LC} and IR_{FV} with favorable clinical scores.

1. Introduction

Osteonecrosis of the femoral head often occurs in patients under the age of 50 years, and causes subchondral collapse which progresses to secondary osteoarthritis (Mankin, 1992). Transtrochanteric rotational osteotomy (Sugioka, 1978) is one of the preferred treatment options for young patients with early post-collapse stages of osteonecrosis of the femoral head. During transtrochanteric rotational osteotomy, the intact area of the femoral head is transposed to the weight-bearing surface by rotation, or varus angulation of the proximal fragment.

The ratio of the transposed intact area of the femoral head to the weight-bearing surface of the acetabulum (intact ratio: IR) on

* Corresponding author at: Department of Mechanical and Aerospace Engineering, University of Florida, 330 MAE-A, P.O. Box 116250, Gainesville, FL 32611-6250, USA.

E-mail addresses: dhara@ortho.med.kyushu-u.ac.jp (D. Hara), hamachan@ortho.med.kyushu-u.ac.jp (S. Hamai), krmiller678@ufl.edu (K.R. Miller), goromoto@ortho.med.kyushu-u.ac.jp (G. Motomura), yoshi134@ortho.med.kyushu-u.ac.jp (K. Yoshimoto), kkomi@ortho.med.kyushu-u.ac.jp (K. Komiyama), k-shio@ortho.med.kyushu-u.ac.jp (K. Shiomoto), sikemura@ortho.med.kyushu-u.ac.jp (S. Ikemura), yasunaka@ortho.med.kyushu-u.ac.jp (Y. Nakashima), banks@ufl.edu (S.A. Banks).

https://doi.org/10.1016/j.clinbiomech.2021.105284
Received 23 August 2020; Accepted 22 January 2021
Available online 26 January 2021

anteroposterior radiographs is significantly associated with progressive collapse, osteoarthritic change, and clinical outcomes (Miyanishi et al., 2000; Motomura et al., 2012; Sugioka et al., 1982; Yamamoto et al., 2010a). Although static IR in multi-planes has been assessed using two-dimensional (2D) magnetic resonance images (MRI) (Ha et al., 2010; Kubo et al., 2017), three-dimensional (3D) changes of IR during dynamic weight-bearing activity are still unknown. Especially in hips after anterior rotational osteotomy, the necrotic lesion moves into the acetabulum during activities requiring deep hip flexion, such as chair-rising and squatting, which may affect progressive collapse, osteoarthritic change, and clinical outcomes. Additionally, the 3D localization of necrotic lesion before and after transtrochanteric rotational osteotomy also may affect dynamic changes of 3DIR and clinical outcomes.

The purpose of this study, therefore, was to quantify hip kinematics and changes in dynamic 3DIR during rising from a chair (chair-rising) and a deep squat (squatting) in patients before and after anterior rotational osteotomy using new methods. Specifically, the following questions were addressed: (1) How does anterior rotational osteotomy change the hip kinematics and 3DIR? (2) How does 3DIR alter during weight-bearing activities preoperatively and postoperatively? and (3) What factors including clinical scores and localization of the necrotic lesion have correlations with 3DIR?

2. Methods

2.1. Patient demography

We reviewed consecutive nine hips in seven patients who underwent anterior rotational osteotomy for symptomatic osteonecrosis of the femoral head by two surgeons between July 2012 and September 2016. Among them, eight hips in six patients satisfied all inclusion criteria, which were (1) no previous surgery in hip joints, other joints, or spine, (2) no osteoarthritic change in bilateral hip joint. All patients were male, with the mean age of 36 years (standard deviation [SD] 12, range, 17–53), the mean height of 172 cm (SD 7, range, 165–184), the mean weight of 68 kg (SD 2, range, 65–72), the mean body mass index of 23 kg/m^2 (SD 2, range, 19–25), and the mean postoperative follow-up period of 28 months (SD 14, range, 13–55). The diagnosis of osteonecrosis of the femoral head was based on the clinical presentation and imaging studies, including plain radiographs and the findings of MRI (Sugano et al., 1999). The etiology of osteonecrosis of the femoral head involved corticosteroids in five hips and alcohol abuse in three hips. According to the classification of the Japanese Investigation Committee of Health and Welfare (Sugano et al., 2002), six hips were classified as stage 3A (which indicates the collapse of the femoral head to be less than 3 mm), and two hips were classified as stage 3B (with 3 mm or more of the collapse). The location of the necrotic lesion was type C2 (the necrotic lesion occupies more than two-thirds of the region and extends to the acetabular edge) in all eight hips. The Harris hip score (Harris, 1969) was recorded before surgery and at the final follow-up. After being informed of the risks associated with radiation exposure, all six patients (eight hips) preoperatively provided their informed consent to participate in this Institutional Review Board-approved study (approval number: 25–55 and 27–404, Kyushu University, Fukuoka, Japan). The data were handled following the ethical standards of the Helsinki Declaration of 1975, as revised in 2000. Pre- and post-operative data acquisitions were performed within one month before surgery, and at the final follow-up period of mean 28 months (SD 14, range, 13–55).

2.2. Operative protocol

Anterior rotational osteotomy was indicated for patients in whom one-third or more of the posterior surface was intact on a lateral view radiograph of the femoral head (Sugioka et al., 1982), For all surgeries, patients were placed in the lateral decubitus position. The surgical procedures were performed according to previously described methods (Sugioka, 1978; Yamamoto et al., 2010a, 2014). Anterior rotational osteotomy was performed in the following order: (1) osteotomy of the greater trochanter, (2) intertrochanteric osteotomy from superolateral to inferomedial on the anteroposterior view (first osteotomy), (3) osteotomy from the proximal flare of the lesser trochanter toward the inferomedial extent of the intertrochanteric osteotomy (second osteotomy), and (4) anterior rotation of the proximal fragment. When the expected postoperative intact ratio on plain radiograph was less than 40%, we inclined the first osteotomy intraoperatively to increase the varus angulation.

After rotation of the proximal fragment, a K-MAX Adjustable Angle Hip Screw (K-MAX AA Hip Screw; Kyocera, Osaka, Japan) and one or two other cancellous bone screws were used to obtain rigid fixation of the osteotomy site under fluoroscopic control (Ikemura et al., 2007). Wheelchair use began 2 days after surgery, and passive range-of-motion exercises began 5 days after surgery. Patients were transferred to another rehabilitation hospital 2 weeks after surgery. Non-weight-bearing was continued until 5 weeks after surgery, at which time the patients were allowed to engage in partial weight-bearing. Full weight-bearing was permitted approximately 4 to 6 months after surgery.

2.3. Image acquisition and 3D modeling

All radiographic images were acquired using a flat panel X-ray detector (Ultimax-I, Toshiba, Tochigi, Japan) with an image area of 420 mm (H) × 420 mm (V) and 0.274 mm × 0.274 mm/pixel resolution preoperatively and postoperatively. For neutral standing, a one-shot radiograph was acquired in a relaxed standing position with the toes facing forward. Periodic radiographic images were acquired for chair-rising and squatting. The frame rate was set at 3.5 frames/s to acquire high-resolution images. For chair-rising, patients rose from a seated position on a chair of 46.5-cm height. For squatting, patients stood from a position with maximum hip flexion (Hara et al., 2014, 2016). This protocol provided an average of 14 images per chair-rise and 12 images per squat activity.

Each subject underwent computed tomography (CT; Aquilion, Toshiba, Tochigi, Japan) preoperatively and postoperatively with a standard protocol (Hara et al., 2016, 2014). With reference to the pre- and post-operative MRI images, the CT images were segmented, and 3D surface models of the necrotic lesion of the femoral head, intact femur, whole femur, implants (only postoperative hips), and pelvis were created using open-source segmentation software (ITK-SNAP, Penn Image Computing and Science Laboratory, Philadelphia, PA, USA) (Yushkevich et al., 2006). Anatomical coordinate systems of the pelvis and femur were embedded in the bone model derived from CT data systems using commercial software (Geomagic Studio 2014, Raindrop Geomagic, Research Triangle Park, Morrisville, NC, USA). The coordinate system of the pelvis was based on the anterior pelvic plane (Hara et al., 2014), and the origin was determined as the center of a best-fit sphere to the acetabulum (Sato et al., 2017). The coordinate system of the femur was based on the International Society of Biomechanics recommendation (Hara et al., 2014; Sato et al., 2017).

2.4. Model-image registration

Hip joint kinematics were quantified using open-source software for 3D-to-2D model-image registration (JointTrack, www.sourceforge.net/projects/jointtrack) (Banks and Hodge, 1996; Kawahara et al., 2020; Sato et al., 2017). The bone model was projected onto the fluoroscopic image, and its three-dimensional pose was iteratively adjusted to match its silhouette with the silhouette of the fluoroscopic image. The accuracy of this method for the hip was 0.2 mm for in-plane translation, 0.5 mm for out-of-plane translation, and 1.6° for rotations (Sato et al., 2017).

2.5. Geometric analysis

Using Geomagic Studio and custom MATLAB programs (MathWorks, Inc., Natick, MA, USA), we measured preoperative and postoperative angles three-dimensionally described as the following: (1) neck-shaft angle: the angle between the femoral neck axis and the femoral shaft axis in the coronal plane and (2) anteversion angle: the angle between the femoral neck axis and the transepicondylar axis in the axial plane (Akiyama et al., 2012).

2.6. Data processing

The relative positions and orientations of the femur to the pelvis were defined as hip movements (Hara et al., 2014). Hip movements were determined using the Cardan/Euler angle system in x-z-y order (flexion/extension, adduction/abduction, and internal/external) (Kadaba et al., 1990; Koyanagi et al., 2011).

The original two-dimensional intact ratio (2DIR) was measured according to the previously described method using the preoperative and postoperative radiographs during neutral standing (Fig. 1) (Sugioka et al., 1982). The femoral head was divided into octants by three planes intersecting at the center of the femoral head (Fig. 2), namely Anterior Superior Lateral (ASL), Anterior Superior Medial (ASM), Anterior Inferior Lateral (AIL), Anterior Inferior Medial (AIM), Posterior Superior Lateral (PSL), Posterior Superior Medial (PSM), Posterior Inferior Lateral (PIL) and Posterior Inferior Medial (PIM) (Bassounas et al., 2007). Then, the surface areas of each octant of the femoral head ($Area_{OFH}$) and the necrotic lesion ($Area_{ONL}$) were measured using Geomagic Studio. The 3DIR in the octant (IR_{OCT}) was expressed as 100*($Area_{OFH}$ - $Area_{ONL}$)/$Area_{OFH}$.

To describe the dynamic 3DIR we used two methods, namely the lunate coverage method and force vector method. For these two methods, the bone surface models of the lunate, whole femoral head, and necrotic lesion were extracted using a Geomagic Studio. For the lunate coverage method, the 3D kinematics of these models in each frame were visualized in Geomagic Studio. In all frames, the contour of the lunate was projected onto the nearest surfaces of the whole femoral head and necrotic lesion to create the boundaries of acetabular coverage, respectively (Hansen et al., 2012). Then, the lunate boundary covered the area of the whole femoral head ($Area_{LCFH}$) and necrotic lesion ($Area_{LCNL}$) were computed automatically (Fig. 3a). The 3D intact ratio by the lunate coverage method (IR_{LC}) was expressed as 100*($Area_{LCFH}$ - $Area_{LCNL}$)/$Area_{LCFH}$ (Fig. 3b).

For the force vector method, the peak contact force vector was determined according to the dataset of a previous study demonstrating the direction of contact force through the *in vivo* hip joint during chair-rising (Bergmann et al., 2001). Along the peak contact force vector, the contact force cylinder was determined (Fig. 3c). Because a previous study (Yoshida et al., 2006) using the dataset for the direction of contact force through the *in vivo* hip joint during chair-rising (Bergmann et al., 2001) demonstrated that the corresponding contact area was 19.7% of the lunate area when the contact force showed the highest value during chair-rising, we set the radius of the contact force cylinder to the value which was the same as that of a circle whose area was 19.7% of the lunate area. The weight-bearing surface of the lunate (WBS_L, Fig. 3c) was defined as the region that was intersected by the contact force cylinder. The weight-bearing surfaces of the whole femoral head (WBS_{FH}) and the necrotic lesion (WBS_{NL}) were defined as the regions that were intersected by the projection of WBS_L along the peak contact force vector in the whole femoral head and the necrotic lesion, respectively (Fig. 3c). Then, the area of WBS_{FH} ($Area_{WBSFH}$) and WBS_{NL} ($Area_{WBSNL}$) were computed. These procedures were automatically performed using a custom MATLAB program. The 3D intact ratio by the force vector method (IR_{FV}) was expressed as 100*($Area_{WBSFH}$ - $Area_{WBSNL}$)/$Area_{WBSFH}$ (Fig. 3d).

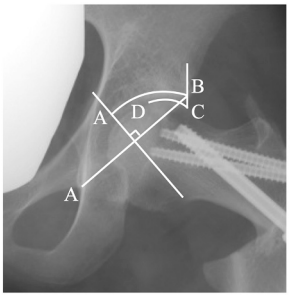

$$\text{2D intact ratio} = \frac{\text{C–D}}{\text{A–B}} \times 100\ (\%)$$

Fig. 1. The original 2D intact ratio. The 2D intact ratio is determined using an anteroposterior radiograph during neutral standing and is expressed as the length ratio of the intact articular surface of the femoral head (C–D) to the weight-bearing surface of the acetabulum (A–B). Point A is determined by drawing a perpendicular line from the midpoint between point B (the lateral edge of the acetabulum) and E (the lowest point of the teardrop) to the acetabulum. Points C and D show the lateral edge of the weight-bearing surface and the medial edge of the intact articular surface, respectively.

2.7. Statistical analysis

Values were expressed as means (SD). Statistical analyses were performed using JMP Pro Version 15.0 (SAS Institute, Cary, NC, USA). All data were tested for normality with the Shapiro-Wilk test. To compare static IRs, Harris hip score, and geometry between preoperative and postoperative hips, paired *t*-test or Wilcoxon signed-rank test was used as appropriate. Two-way (%movement cycle x group) repeated measures analysis of variance (RMANOVA) was also used to compare hip kinematics and dynamic 3DIRs during the motion between preoperative and postoperative hips. Correlation among parameters were examined with Pearson's correlation coefficients or Spearman's rank correlation coefficients as appropriate. Because two patients (two hips) could not achieve preoperative squatting due to hip discomfort and instability during the motion, these two hips were excluded from the analysis during squatting for pair-wise comparison. The significance level was set at $P < 0.05$ for all tests except multiple comparisons for correlation among parameters. Multiple comparisons were accounted for by using a false discovery rate (Glickman et al., 2014) adjustment $\alpha = 0.05$ (Jankovic et al., 1990).

3. Results

3.1. Harris hip score and hip geometry

Harris hip score significantly improved from 67 (10, range 57–79) preoperatively to 90 (6, range 81–100, $P < 0.001$). Neck-shaft and anteversion angles significantly decreased from 120° (8, range 111–127) and 5° (12, range − 10 to 29) preoperatively to 114° (4, range 109–120, $P = 0.03$) and − 6° (14, range − 26 to 15, $P = 0.02$) postoperatively, respectively.

3.2. Hip kinematics

For chair-rising (Fig. 4a), the maximum hip flexion angles during the full movement cycle were 82° (18, range 55–110) preoperatively and 75° (13, range 55–97) postoperatively. RMANOVA showed no significant differences in hip flexion/extension, hip adduction/abduction, or hip internal/external rotation between preoperative and postoperative hips ($P = 0.19$, 0.76, and 0.21, respectively), and there were no significant interactions (Fig. 4a–c).

In squatting (Fig. 4d), the maximum hip flexion angles were 92° (9, range 78–104) preoperatively and 81° (14, range 58–96) postoperatively. RMANOVA showed no significant differences in hip flexion/extension, hip adduction/abduction, or hip internal/external rotation between preoperative and postoperative hips ($P = 0.72$, 0.87,

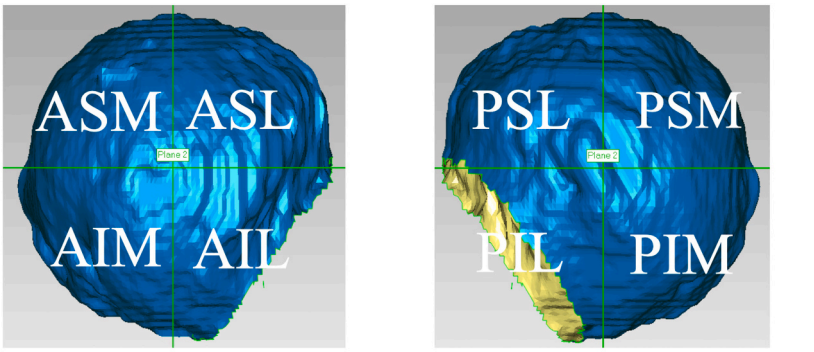

Fig. 2. The 3DIR in the octant (IR_{OCT}) After extracting the bone model of the femoral head from the whole femur bone model, the femoral head was divided into octants by three planes intersecting at the center of the femoral head, namely Anterior Superior Lateral (ASL), Anterior Superior Medial (ASM), Anterior Inferior Lateral (AIL), Anterior Inferior Medial (AIM), Posterior Superior Lateral (PSL), Posterior Superior Medial (PSM), Posterior Inferior Lateral (PIL) and Posterior Inferior Medial (PIM) (Bassounas et al., 2007). Then, The 3DIR in the octant (IR_{OCT}) was measured as the ratio of the surface area of each octant of the femoral head and the necrotic lesion.

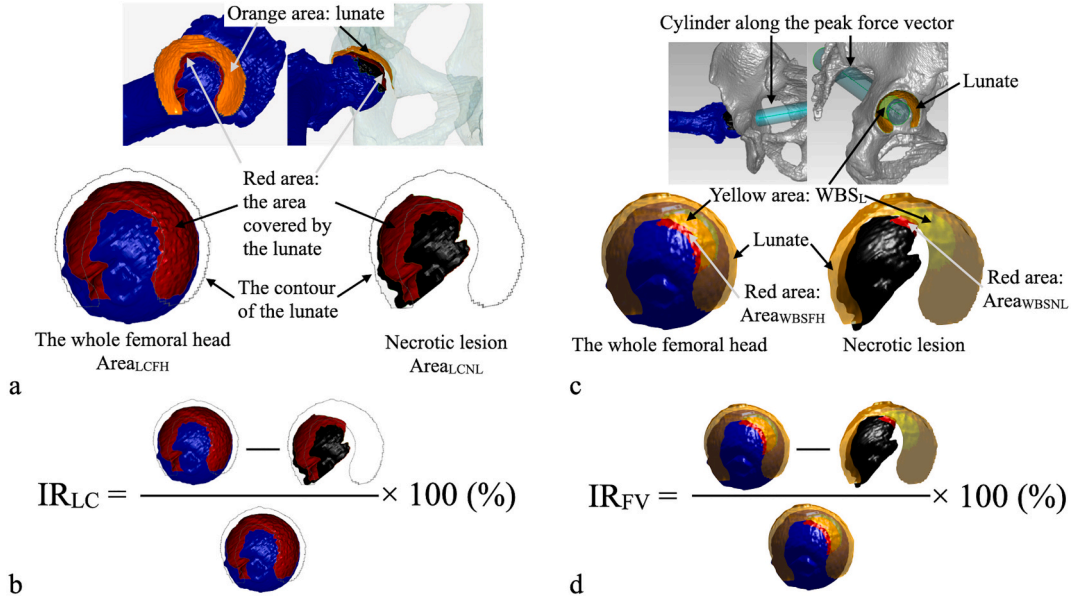

Fig. 3. Three-dimensional intact ratio by lunate coverage method (IR_{LC}) and force vector method (IR_{FV}). (a) The lunate covered area of the whole femoral head ($Area_{LCFH}$) and necrotic lesion ($Area_{LCNL}$) were marked and computed automatically using Geomagic Studio. (b) IR_{LC} was expressed as 100*($Area_{LCFH}$ - $Area_{LCNL}$)/$Area_{LCFH}$). (c, upper panels) The weight-bearing surface of the lunate (WBS_L, yellow area) was defined as the lunate region (right: orange area) that was intersected by the contact force cylinder (green cylinder) which was determined according to the dataset of the previous study (Bergmann et al., 2001; Yoshida et al., 2006). (d, lower panels) The areas of the weight-bearing surface of the whole femoral head ($Area_{WBSFH}$, left: red area) and necrotic lesion ($Area_{WBSNL}$, right: red area) were computed as the areas that were intersected by the projection of WBS_L (left and right: transparent yellow area) along the contact force cylinder in the whole femoral head (left: purple area), and necrotic lesion (right: black area), respectively.
(d) IR_{FV} was expressed as 100*($Area_{WBSFH}$ - $Area_{WBSNL}$)/$Area_{WBSFH}$. (For interpretation of the references to colour in this figure legend, the reader is referred to the web version of this article.)

and 0.18 respectively), and there were no significant interactions (Fig. 4d–f).

3.3. Intact ratio

The necrotic lesion was generally located toward the anterosuperior region of the femoral head preoperatively, and anteromedial region postoperatively (Table 1). The mean IR_{OCT} in ASL PSL, and PSM significantly increased preoperatively to postoperatively (P = 0.008, 0.008, and 0.01, respectively), whereas the mean IR_{OCT} in AIM and PIM significantly decreased (P = 0.001 and 0.008, respectively). Additionally, these five IR_{OCT}s (ASL, AIM, PSL, PSM, and PIM) had significant correlations with Harris hip score (Table 2).

During neutral standing, both 2DIR, IR_{LC}, and IR_{FV} significantly increased from 1% (2, range 0–6), 50% (8, range 34–63), and 4% (4, range 0–10) preoperatively to 54% (14, range 40–85), 74% (4, range 68–79), and 72% (15, range 47–94) postoperatively, respectively (P = 0.008, < 0.001, and 0.008, respectively). Seven parameters had significant correlations with 2DIR, IR_{LC}, and IR_{FV} during standing, including Harris hip score and IR_{OCT} in ASL, ASM, AIM, PSL, PSM, and PIM (Table 2). Additionally, 2DIR had significant correlations with both IR_{LC} and IR_{FV} during neutral standing (Table 2).

When chair-rising (Fig. 5a and b), IR_{LC} and IR_{FV} averaged 42% (10, range 27–53) and 7% (4, range 1–14) preoperatively, and 66% (10, range 52–76) and 79% (13, range 58–94) postoperatively, respectively. RMANOVA showed that both IR_{LC} and IR_{FV} significantly increased from preoperatively to postoperatively (P < 0.001 and < 0.001 respectively) without any interactions. Additionally, RMANOVA also showed that both IR_{LC} and IR_{FV} significantly changed during the chair-rise motion (P < 0.001 and 0.02, respectively, Fig. 5a and b). In particular, the mean postoperative IR_{LC} at maximum hip flexion (56% [16, range 33–75]) was significantly smaller than that at minimum hip flexion (77% [4, range 70–82], mean difference: 20 [95% confidence intervals {CI}: 8–33], P = 0.006). However, no significant difference was found

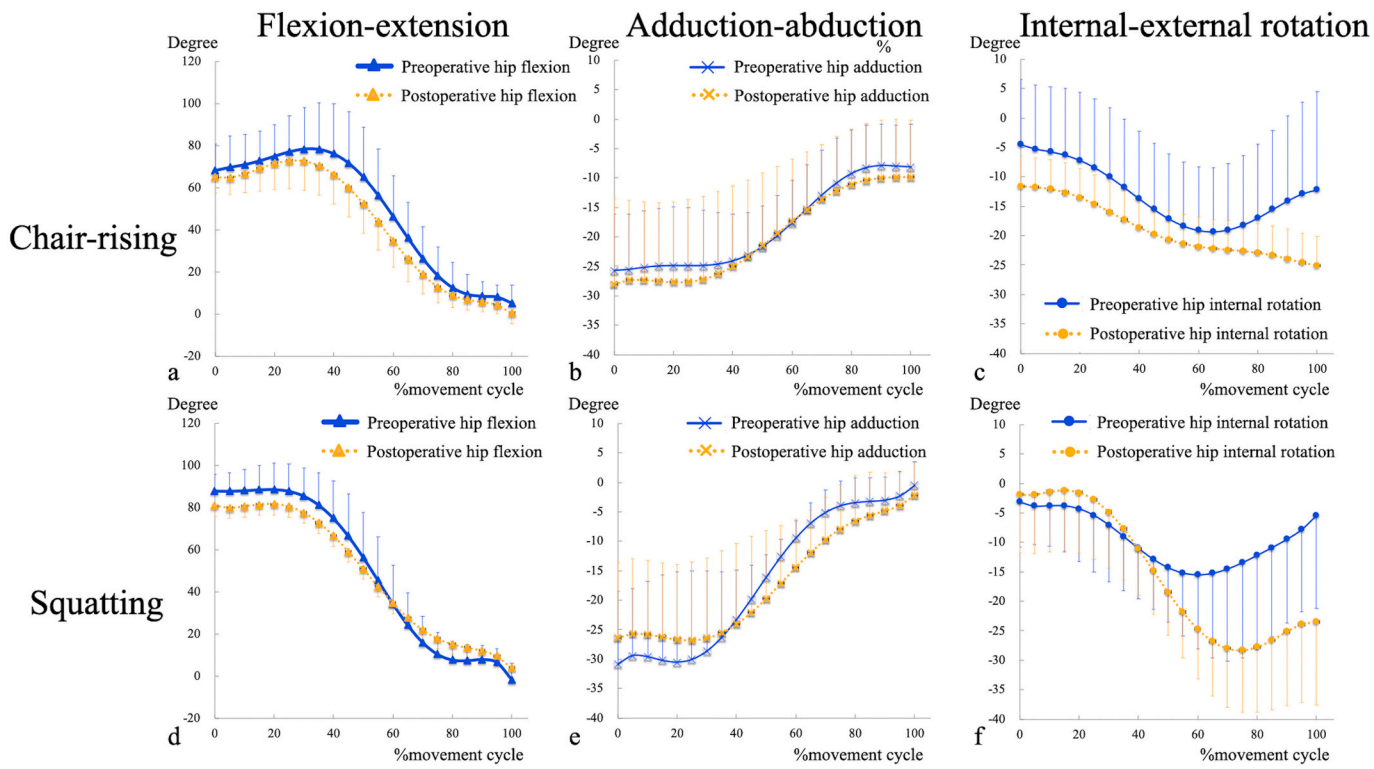

Fig. 4. The mean hip kinematics. Hip flexion-extension (a), adduction-abduction (b), internal-external rotation (c) during chair-rising. Hip flexion-extension (d), adduction-abduction (e), internal-external rotation (f) during squatting.

Table 1
Comparison of IR_{OCT} between preoperative and postoperative hips.

Parameters	Preoperative	Postoperative	Mean difference (95%CI)	*P* value
IR_{OCT} in ASL (%)	35 (22)	86 (21)	51 (30–72)	*0.008*†
IR_{OCT} in ASM (%)	15 (21)	28 (13)	13 (−6 to 33)	0.20†
IR_{OCT} in AIL (%)	88 (11)	87 (19)	−2 (−21 to 17)	0.69†
IR_{OCT} in AIM (%)	82 (18)	33 (15)	−49 (−71 to −27)	*0.001**
IR_{OCT} in PSL (%)	76 (27)	100 (0)	24 (9–46)	*0.008*†
IR_{OCT} in PSM (%)	54 (12)	79 (18)	24 (8–40)	*0.01**
IR_{OCT} in PIL (%)	100 (0)	100 (0)	0	1.0†
IR_{OCT} in PIM (%)	98 (5)	82 (14)	−16 (−28 to −4)	*0.03*†

Values are expressed as means (standard deviation) in preoperative and postoperative parameters. *P* values < 0.05 were considered statistically significant. IR_{OCT}: three-dimensional intact ratio in the octant, CI: confidence intervals, ASL: Anterior Superior Lateral, ASM: Anterior Superior Medial, AIL: Anterior Inferior Lateral, AIM: Anterior Inferior Medial, PSL: Posterior Superior Lateral, PSM: Posterior Superior Medial, PIL: Posterior Inferior Lateral and PIM: Posterior Inferior Medial.

* Paired *t*-test.

† Wilcoxon signed-rank test, significant values are italicized.

between the mean postoperative IR_{FV} at maximum hip flexion (83% [15, range 58–99]) and that at minimum hip flexion (73% [15, range 49–94], mean difference: 10 [95%CI: −0.8 to 21], $P = 0.06$). Five parameters had significant correlations with both the mean IR_{LC} and IR_{FV} during chair-rising, including Harris hip score, 2DIR, and IR_{OCT} in ASL, ASM, and PSL (Table 2).

During squatting (Fig. 5c and d), IR_{LC} and IR_{FV} averaged 41% (12%, range 22–53) and 4% (4, range 0–11) preoperatively, and 65% (10, 51–76) and 77% (14, range 57–97) postoperatively, respectively. RMANOVA showed that both IR_{LC} and IR_{FV} increased from preoperatively to postoperatively ($P = 0.002$ and < 0.001 respectively) without any interactions. Additionally, RMANOVA also showed that IR_{LC} significantly changed during the squatting motion ($p = 0.04$, Fig. 5c). In particular, the mean postoperative IR_{LC} at maximum hip flexion (57% [18, range 36–76]) was significantly smaller than that at minimum hip flexion (75% [4, range 68–80], mean difference: 23 [95%CI: 5–41], $P = 0.02$). However, IR_{FV} did not significantly change during the squatting motion ($P = 0.12$, Fig. 5d). Five parameters had significant correlations with both the mean IR_{LC} and IR_{FV} during squatting, including Harris hip score, anteversion angle, 2DIR, and IR_{OCT} in ASL, PSL, and PIM (Table 2).

4. Discussion

To our knowledge, this is the first *in vivo* study examining the changes in dynamic 3DIR and kinematics of hips with osteonecrosis of the femoral head during weight-bearing activities including deep hip flexion before and after anterior rotational osteotomy. Anterior rotational osteotomy did not significantly change the hip kinematics but significantly increased both IR_{LC} and IR_{FV} as with Harris hip score. Overall, IR_{LC} significantly changed during the motion whereas IR_{FV} did not. Both IR_{LC} and IR_{FV} were significantly correlated with Harris hip score, 2DIR, and IR_{OCT} mainly in the superolateral regions. Greater 3DIRs correlated with better clinical outcomes.

Preoperative hips with osteonecrosis of the femoral head showed similar kinematics to healthy hips (Hara et al., 2014; Hemmerich et al., 2006; Spyropoulos et al., 2013) and larger range of motions than hips with osteoarthritis (Eitzen et al., 2014; Hara et al., 2016) during both chair-rising and squatting (the mean maximum hip flexion: 79°/84–86°/60–64° during chair-rising and 91°/95–102°/68° during squatting in

Table 2
Correlations among parameters.

		Neutral standing			Chair-rising		Squatting	
Parameters	Harris hip score	2DIR	IR_{LC}	IR_{FV}	Mean IR_{LC}	Mean IR_{FV}	Mean IR_{LC}	Mean IR_{FV}
Harris hip score	–	*0.73*†	*0.84**	*0.81*†	*0.78**	*0.77*†	*0.76**	*0.75*†
Neck-shaft angle	*−0.61**	−0.48†	*−0.60**	*−0.73*†	−0.48*	*−0.66*†	−0.52*	−0.46†
Anteversion angle	−0.57*	−0.48†	−0.49*	−0.44†	*−0.68**	−0.44†	*−0.73**	*−0.62*†
2DIR	*0.73*†	–	*0.80*†	*0.83*†	*0.84*†	*0.83*†	*0.85*†	*0.86*†
IR_{OCT} in ASL	*0.69**	*0.75*†	*0.76**	*0.76**	*0.89**	*0.78**	*0.89**	*0.78**
IR_{OCT} in ASM	0.33*	*0.58*†	*0.55**	*0.54*†	*0.58**	*0.52*†	0.59*	0.39*
IR_{OCT} in AIL	−0.02†	0.20†	−0.01†	−0.02†	0.38†	−0.01†	0.35†	0.20†
IR_{OCT} in AIM	*−0.72**	*−0.68*†	*−0.72**	*−0.79**	−0.46*	*−0.80**	−0.44*	*−0.79**
IR_{OCT} in PSL	*0.86*†	*0.79*†	*0.76*†	*0.82*†	*0.69*†	*0.73*†	*0.70*†	*0.77*†
IR_{OCT} in PSM	*0.53**	*0.57*†	*0.73**	*0.73*†	0.39*	*0.63**	0.43*	0.45†
IR_{OCT} in PIL	–	–	–	–	–	–	–	–
IR_{OCT} in PIM	*−0.68*†	*−0.54*†	*−0.52*†	*−0.63*†	*−0.64*†	−0.60†	*−0.65*†	*−0.72*†

Multiple comparisons were accounted for by using a false discovery rate (Glickman et al., 2014) adjustment α = 0.05 (Jankovic et al., 1990). Both preoperative and postoperative hips were included in the analysis.
IR_{LC}: three-dimensional intact ratio by lunate coverage method, IR_{FV}: three-dimensional intact ratio by force vector method, IR_{OCT}: three-dimensional intact ration in the octant, ASL: Anterior Superior Lateral, ASM: Anterior Superior Medial, AIL: Anterior Inferior Lateral, AIM: Anterior Inferior Medial, PSL: Posterior Superior Lateral, PSM: Posterior Superior Medial, PIL: Posterior Inferior Lateral and PIM: Posterior Inferior Medial.
* Pearson's correlation coefficients.
† Spearman's rank correlation coefficients, Significant values are italicized.

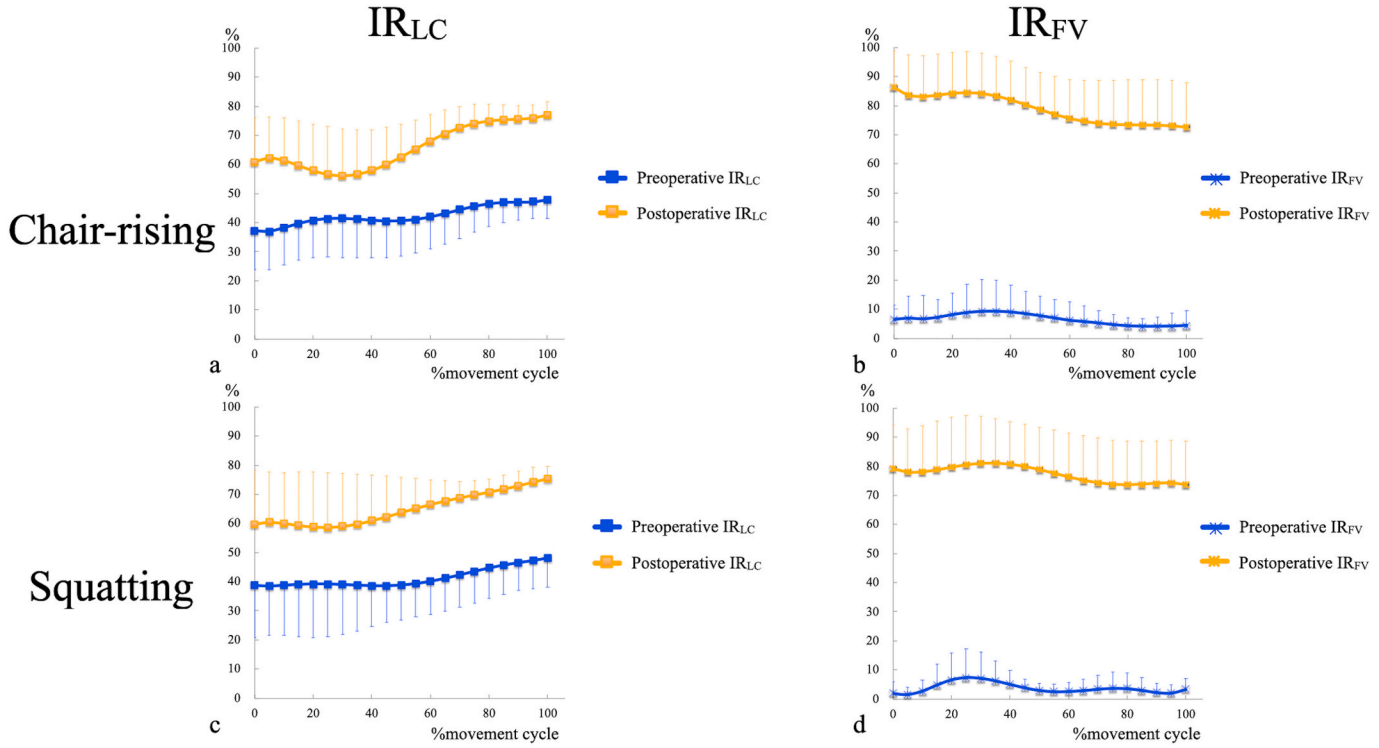

Fig. 5. The mean three-dimensional intact ratios. IR_{LC} (a) and IR_{FV} (b) during chair-rising. IR_{LC} (c) and IR_{FV} (d) during squatting. IR_{LC}: three-dimensional intact ratio by lunate coverage method, IR_{FV}: three-dimensional intact ratio by force vector method.

osteonecrosis of the femoral head /healthy/osteoarthritic hips, respectively). In this study, preoperative hips with osteonecrosis of the femoral head maintained ranges of motion probably due to little osteoarthritic change. Additionally, postoperative hip kinematics did not significantly differ from preoperative hip kinematics during both chair-rising and squatting. Anterior rotational osteotomy has advantages of not only preserving the native joints and but also ranges of motion with favorable clinical outcomes as shown in previous studies (Yamamoto et al., 2010a, 2010b; Yoon et al., 2008). These kinematic results may be useful for surgeons and patients with symptomatic osteonecrosis of the femoral head without osteoarthritic change to decide whether to undergo anterior rotational osteotomy or other surgeries.

IR_{LC} assessed dynamic changes of 3DIR geometrically. IR_{LC} during all activities was also correlated with Harris hip score and 2DIR. As reported in previous studies using plain radiographs (Kubo et al., 2017; Miyanishi et al., 2000; Sonoda et al., 2015; Zhao et al., 2013), clinical scores are affected by multiple factors such as degree and location of collapse, and osteoarthritic change as well as IR which is also associated with progressive collapse and osteoarthritic change. Our results indicate that substantial postoperative IR_{LC} may be important to achieve better clinical results by preventing progressive collapse as with 2DIR (Miyanishi et al., 2000; Sonoda et al., 2015; Zhao et al., 2013). Postoperative IR_{LC} significantly decreased as hip flexion angle increased during both chair-rising and squatting, which is reasonable because the

anteromedially transposed necrotic lesion moved into the lunate during deep hip flexion. Indeed, IR_{OCT} in ASM had a significant positive correlation with IR_{LC} during chair-rising. Sugioka and Yamamoto (2008) pointed out that the repetition of the collapsed necrotic lesion moving into and out of the lunate might damage the lunate articular surface. Thus, posterior rotational osteotomy may be better to keep substantial IR_{LC} during hip flexion than anterior rotational osteotomy in terms of IR (Sugioka et al., 1982), as reported in a previous study using 2DIR 45° of hip flexion (Atsumi, 2006).

IR_{FV} assessed the dynamic change of 3DIR in the region in which the peak contact forces are applied (Bergmann et al., 2001). As with IR_{LC}, IR_{FV} during all activities was also correlated with Harris hip score and 2DIR, which indicates that achieving substantial postoperative IR_{FV} may lead to excellent clinical results by preventing progressive collapse. No overlaps were found in IR_{FV} during motion in any hips comparing preoperative and postoperative values. Additionally, substantial postoperative IR_{FV} was maintained throughout the motion. These results show IR_{FV} is not strongly influenced by hip movement but depends more on geometric factors like IR_{OCT}. When substantial IR_{FV} is achieved in the neutral position, activities with deep hip flexion may be acceptable after femoral osteotomy because there is substantial intact bone occupying the region where peak contact forces are applied.

To achieve sufficient postoperative IR_{LC} and IR_{FV}, transposition of the necrotic lesion from the superolateral to the inferomedial region is important. Both IR_{LC} and IR_{FV} had positive correlations with IR_{OCT} mainly in the superolateral region, and negative correlations with IR_{OCT} mainly in the inferomedial region. A previous study demonstrated that the direction of contact force through the *in vivo* hip joint during chair-rising was around the superomedial region (Bergmann et al., 2001). Thus, increasing IR_{OCT} at regions apart from the superomedial region such as the inferomedial region may be effective to reduce the contact forces to the necrotic lesion. Additionally, these results may be helpful for the assessment of the transposed intact area during surgeries. Decreasing neck-shaft angle, *i.e.* varus angulation, was also significantly correlated with 2DIR, IR_{LC}, and IR_{FV} during neutral standing in this study, as with the previous study using 2DIR (Miyanishi et al., 2000; Sugioka et al., 1982). Preoperative 3D simulation (Sonoda et al., 2017) may be useful to achieve adequate postoperative 2DIR and 3DIRs (IR_{LC} and IR_{FV}).

This study has several limitations. First, we were limited by the small number of male patients. Further studies are necessary. However, the number of patients in this study is similar to that in previous hip kinematic studies (7–8 hips with osteoarthritis which is more common than osteonecrosis of the femoral head) (Komiyama et al., 2019; Tsai et al., 2015). Second, sequential movements were collected twice because even the large flat-panel X-ray detector provided a limited field of view. Third, surface bone models were derived from CT, not MRI, which might make the segmentation of the necrotic lesion imprecise. However, CT can accurately display the characterization of the necrotic lesion (Barille et al., 2014; Hu et al., 2015; Marker et al., 2011), and CT images were segmented with reference to MRI images in order not to misidentify the lesion. Moreover, all hips were classified as stage 3A or 3B in this study, which indicates that the collapse of the femoral head and sclerotic bands were clear. Fourth, 3D collapse quantification was not performed in this study because no reliable methods have been developed. Further studies are needed. Finally, the peak contact force vector was derived from a previous study (Bergmann et al., 2001) in which hip geometries such as neck-shaft angle or anteversion angle may be different from those in this study. However, very few studies have examined hip contact forces *in vivo*, and we believe that the *in vivo* contact force vector should be taken into account to define the accurate weight-bearing surface during dynamic motions.

5. Conclusions

Hip kinematics were maintained during both chair-rising and squatting with significantly improved Harris hip score after anterior rotational osteotomy. Anterior rotational osteotomy significantly increased 2DIR, IR_{LC}, and IR_{FV}. Additionally, both IR_{LC} and IR_{FV} had significant correlations with Harris hip score, 2DIR, and IR_{OCT} in mainly superolateral regions among both preoperative and postoperative hips. To reduce the contact forces to the necrotic lesion, increasing IR_{OCT} at regions apart from the superior regions such as the inferomedial region may be effective. Overall, postoperative IR_{LC} decreased as the hip flexion angle increased. However, postoperative IR_{FV} was relatively constant during deep flexion, suggesting that substantial intact bone occupies the contacting region across the entire motion if adequate IR_{FV} is achieved in the neutral standing position. These results may be helpful for preoperative planning, feedback to surgeons, and achieving better clinical outcomes.

Author contributions

DH, SH, YN, and SAB contributed to the conception and design of the study; DH, SH, KY, KK, and KS performed acquisition of data; DH, KRM, SAB conducted data analysis; DH, SH, GM, SI, YN, and SAB contributed to data interpretation; and preparation of the manuscript. All authors contributed to revising the draft and approved the final version of the manuscript.

Funding

This work was supported by Japan Society for the Promotion of Science Grant Number 15K10450, a grant from the Japan Orthopaedics and Traumatology Foundation Inc. (No. 263), and a grant from the Nakatomi Foundation.

Conflict of interests

Satoshi Hamai has received speaking fees from Smith & Nephew, Yasuharu Nakashima has received speaking fees from Zimmer and Kyocera, and DePuy Synthes, Scott A. Banks has received royalties, consulting fees or research grants from DJO Surgical, Exactech, Hospital for Special Surgery, Lima, Orthosensor, Smith & Nephew, and Stryker/MAKO Surgical.

Acknowledgments

The authors would like to thank Junji Kishimoto, a statistician from the Digital Medicine Initiative, Kyushu University, for his valuable comments and suggestions regarding statistical analysis, Kazuyuki Karasuyama, Yusuke Kubo, Kazuhiko Sonoda, and Takeshi Utsunomiya from Department of Orthopaedic Surgery, Graduate School of Medical Sciences, Kyushu University, for their valuable suggestions, and Nicholas J. Dunbar and Chin-Chiang Chang from Department of Mechanical and Aerospace Engineering, University of Florida, for their assistance and valuable comments regarding the analysis program.

References

Akiyama, M., Nakashima, Y., Fujii, M., Sato, T., Yamamoto, T., Mawatari, T., Motomura, G., Matsuda, S., Iwamoto, Y., 2012. Femoral anteversion is correlated with acetabular version and coverage in Asian women with anterior and global deficient subgroups of hip dysplasia: a CT study. Skelet. Radiol. 41, 1411–1418. https://doi.org/10.1007/s00256-012-1368-7.

Atsumi, T., 2006. Posterior rotational osteotomy for nontraumatic osteonecrosis with extensive collapsed lesions in young patients. J. Bone Joint Surg. 88, 42–47. https://doi.org/10.2106/JBJS.F.00767.

Banks, S.A., Hodge, W.A., 1996. Accurate measurement of three-dimensional knee replacement kinematics using single-plane fluoroscopy. IEEE Trans. Biomed. Eng. 43, 638–649. https://doi.org/10.1109/10.495283.

Barille, M.F., Wu, J.S., McMahon, C.J., 2014. Femoral head avascular necrosis: a frequently missed incidental finding on multidetector CT. Clin. Radiol. 69, 280–285. https://doi.org/10.1016/j.crad.2013.10.012.

Bassounas, A.E., Karantanas, A.H., Fotiadis, D.I., Malizos, K.N., 2007. Femoral head osteonecrosis: volumetric MRI assessment and outcome. Eur. J. Radiol. 63, 10–15. https://doi.org/10.1016/j.ejrad.2007.03.028.

Bergmann, G., Deuretzbacher, G., Heller, M., Graichen, F., Rohlmann, A., Strauss, J., Duda, G.N., 2001. Hip contact forces and gait patterns from routine activities. J. Biomech. 34, 859–871.

Eitzen, I., Fernandes, L., Nordsletten, L., Snyder-Mackler, L., Risberg, M.A., 2014. Weight-bearing asymmetries during Sit-To-Stand in patients with mild-to-moderate hip osteoarthritis. Gait Posture 39, 683–688. https://doi.org/10.1016/j.gaitpost.2013.09.010.

Glickman, M.E., Rao, S.R., Schultz, M.R., 2014. False discovery rate control is a recommended alternative to Bonferroni-type adjustments in health studies. J. Clin. Epidemiol. 67, 850–857. https://doi.org/10.1016/j.jclinepi.2014.03.012.

Ha, Y.-C., Kim, H.J., Kim, S.-Y., Kim, K.-C., Lee, Y.-K., Koo, K.-H., 2010. Effects of age and body mass index on the results of transtrochanteric rotational osteotomy for femoral head osteonecrosis. J. Bone Joint Surg. 92, 314–321. https://doi.org/10.2106/JBJS.H.01020.

Hansen, B.J., Harris, M.D., Anderson, L.A., Peters, C.L., Weiss, J.A., Anderson, A.E., 2012. Correlation between radiographic measures of acetabular morphology with 3D femoral head coverage in patients with acetabular retroversion. Acta Orthop. 83, 233–239. https://doi.org/10.3109/17453674.2012.684138.

Hara, D., Nakashima, Y., Hamai, S., Higaki, H., Ikebe, S., Shimoto, T., Hirata, M., Kanazawa, M., Kohno, Y., Iwamoto, Y., 2014. Kinematic analysis of healthy hips during weight-bearing activities by 3D-to-2D model-to-image registration technique. Biomed. Res. Int. 2014, 457573–457578. https://doi.org/10.1155/2014/457573.

Hara, D., Nakashima, Y., Hamai, S., Higaki, H., Ikebe, S., Shimoto, T., Yoshimoto, K., Iwamoto, Y., 2016. Dynamic hip kinematics in patients with hip osteoarthritis during weight-bearing activities. Clin. Biomech. 32, 150–156. https://doi.org/10.1016/j.clinbiomech.2015.11.019.

Harris, W.H., 1969. Traumatic arthritis of the hip after dislocation and acetabular fractures: treatment by mold arthroplasty. An end-result study using a new method of result evaluation. J. Bone Joint Surg. Am. 51, 737–755.

Hemmerich, A., Brown, H., Smith, S., Marthandam, S.S.K., Wyss, U.P., 2006. Hip, knee, and ankle kinematics of high range of motion activities of daily living. J. Orthop. Res. 24, 770–781. https://doi.org/10.1002/jor.20114.

Hu, L.B., Huang, Z.G., Wei, H.Y., Wang, W., Ren, A., Xu, Y.Y., 2015. Osteonecrosis of the femoral head: using CT, MRI and gross specimen to characterize the location, shape and size of the lesion. Br. J. Radiol. 88, 20140508. https://doi.org/10.1259/bjr.20140508.

Ikemura, S., Yamamoto, T., Jingushi, S., Nakashima, Y., Mawatari, T., Iwamoto, Y., 2007. Use of a screw and plate system for a transtrochanteric anterior rotational osteotomy for osteonecrosis of the femoral head. J. Orthop. Sci. 12, 260–264. https://doi.org/10.1007/s00776-007-1123-4.

Jankovic, J., McDermott, M., Carter, J., Gauthier, S., Goetz, C., Golbe, L., Huber, S., Koller, W., Olanow, C., Shoulson, I., 1990. Variable expression of Parkinson's disease: a base-line analysis of the DATATOP cohort. The Parkinson Study Group. Neurology 40, 1529–1534. https://doi.org/10.1212/wnl.40.10.1529.

Kadaba, M.P., Ramakrishnan, H.K., Wootten, M.E., 1990. Measurement of lower extremity kinematics during level walking. J. Orthop. Res. 8, 383–392. https://doi.org/10.1002/jor.1100080310.

Kawahara, S., Hara, T., Sato, T., Kitade, K., Shimoto, T., Nakamura, T., Mawatari, T., Higaki, H., Nakashima, Y., 2020. Digitalized analyses of intraoperative acetabular component position using image-matching technique in total hip arthroplasty. Bone Joint Res. 9, 360–367. https://doi.org/10.1302/2046-3758.97.BJR-2019-0260.R2.

Komiyama, K., Hamai, S., Ikebe, S., Yoshimoto, K., Higaki, H., Shiomoto, K., Gondo, H., Hara, D., Wang, Y., Nakashima, Y., 2019. In vivo kinematic analysis of replaced hip during stationary cycling and computer simulation of optimal cup positioning against prosthetic impingement. Clin. Biomech. 68, 175–181. https://doi.org/10.1016/j.clinbiomech.2019.05.035.

Koyanagi, J., Sakai, T., Yamazaki, T., Watanabe, T., Akiyama, K., Sugano, N., Yoshikawa, H., Sugamoto, K., 2011. In vivo kinematic analysis of squatting after total hip arthroplasty. Clin. Biomech. 26, 477–483. https://doi.org/10.1016/j.clinbiomech.2010.11.006.

Kubo, Y., Motomura, G., Ikemura, S., Sonoda, K., Yamamoto, T., Nakashima, Y., 2017. Factors influencing progressive collapse of the transposed necrotic lesion after transtrochanteric anterior rotational osteotomy for osteonecrosis of the femoral head. Orthop. Traumatol. Surg. Res. 103, 217–222. https://doi.org/10.1016/j.otsr.2016.10.019.

Mankin, H.J., 1992. Nontraumatic necrosis of bone (osteonecrosis). N. Engl. J. Med. 326, 1473–1479. https://doi.org/10.1056/NEJM199205283262206.

Marker, D.R., Mont, M.A., Jain, A., Carrino, J.A., 2011. Pitfalls to avoid and advancements to consider for diagnosing hip osteonecrosis on magnetic resonance imaging. Clinic Rev. Bone Miner. Metab. 9, 23–37. https://doi.org/10.1007/s12018-011-9088-4.

Miyanishi, K., Noguchi, Y., Yamamoto, T., Irisa, T., Suenaga, E., Jingushi, S., Sugioka, Y., Iwamoto, Y., 2000. Prediction of the outcome of transtrochanteric rotational osteotomy for osteonecrosis of the femoral head. J. Bone Joint Surg. (Br.) 82, 512–516.

Motomura, G., Yamamoto, T., Nakashima, Y., Yamaguchi, R., Mawatari, T., Iwamoto, Y., 2012. Midterm results of transtrochanteric anterior rotational osteotomy combined with shelf acetabuloplasty for osteonecrosis with acetabular dysplasia: a preliminary report. J. Orthop. Sci. 17, 239–243. https://doi.org/10.1007/s00776-012-0205-0.

Sato, T., Tanino, H., Nishida, Y., Ito, H., Matsuno, T., Banks, S.A., 2017. Dynamic femoral head translations in dysplastic hips. Clin. Biomech. 46, 40–45. https://doi.org/10.1016/j.clinbiomech.2017.05.003.

Sonoda, K., Yamamoto, T., Motomura, G., Nakashima, Y., Yamaguchi, R., Iwamoto, Y., 2015. Outcome of transtrochanteric rotational osteotomy for posttraumatic osteonecrosis of the femoral head with a mean follow-up of 12.3 years. Arch. Orthop. Trauma Surg. 135, 1257–1263. https://doi.org/10.1007/s00402-015-2282-y.

Sonoda, K., Motomura, G., Ikemura, S., Kubo, Y., Yamamoto, T., Nakashima, Y., 2017. Effects of intertrochanteric osteotomy plane and preoperative femoral anteversion on the postoperative morphology of the proximal femur in transtrochanteric anterior rotational osteotomy: 3D CT-based simulation study. Orthop. Traumatol. Surg. Res. 103, 1005–1010. https://doi.org/10.1016/j.otsr.2017.06.012.

Spyropoulos, G., Tsatalas, T., Tsaopoulos, D.E., Sideris, V., Giakas, G., 2013. Biomechanics of sit-to-stand transition after muscle damage. Gait Posture 38, 62–67. https://doi.org/10.1016/j.gaitpost.2012.10.013.

Sugano, N., Kubo, T., Takaoka, K., Ohzono, K., Hotokebuchi, T., Matsumoto, T., Igarashi, H., Ninomiya, S., 1999. Diagnostic criteria for non-traumatic osteonecrosis of the femoral head. A multicentre study. J. Bone Joint Surg. (Br.) 81, 590–595.

Sugano, N., Atsumi, T., Ohzono, K., Kubo, T., Hotokebuchi, T., Takaoka, K., 2002. The 2001 revised criteria for diagnosis, classification, and staging of idiopathic osteonecrosis of the femoral head. J. Orthop. Sci. 7, 601–605. https://doi.org/10.1007/s007760200108.

Sugioka, Y., 1978. Transtrochanteric anterior rotational osteotomy of the femoral head in the treatment of osteonecrosis affecting the hip: a new osteotomy operation. Clin. Orthop. Relat. Res. 191–201.

Sugioka, Y., Yamamoto, T., 2008. Transtrochanteric posterior rotational osteotomy for osteonecrosis. Clin. Orthop. Relat. Res. 466, 1104–1109. https://doi.org/10.1007/s11999-008-0192-9.

Sugioka, Y., Katsuki, I., Hotokebuchi, T., 1982. Transtrochanteric rotational osteotomy of the femoral head for the treatment of osteonecrosis. Follow-up statistics. Clin. Orthop. Relat. Res. 115–126.

Tsai, T.-Y., Dimitriou, D., Li, J.-S., Woo Nam, K., Li, G., Kwon, Y.-M., 2015. Asymmetric hip kinematics during gait in patients with unilateral total hip arthroplasty: in vivo 3-dimensional motion analysis. J. Biomech. 48, 555–559. https://doi.org/10.1016/j.jbiomech.2015.01.021.

Yamamoto, T., Ikemura, S., Iwamoto, Y., Sugioka, Y., 2010a. The repair process of osteonecrosis after a transtrochanteric rotational osteotomy. Clin. Orthop. Relat. Res. 468, 3186–3191. https://doi.org/10.1007/s11999-010-1384-7.

Yamamoto, T., Iwasaki, K., Iwamoto, Y., 2010b. Transtrochanteric rotational osteotomy for a subchondral insufficiency fracture of the femoral head in young adults. Clin. Orthop. Relat. Res. 468, 3181–3185. https://doi.org/10.1007/s11999-010-1364-y.

Yamamoto, T., Ikemura, S., Iwamoto, Y., 2014. Transtrochanteric curved varus osteotomy for the treatment of osteonecrosis of the femoral head. In: Osteonecrosis. Springer, Berlin Heidelberg, Berlin, Heidelberg, pp. 339–344. https://doi.org/10.1007/978-3-642-35767-1_47.

Yoon, T.R., Abbas, A.A., Hur, C.I., Cho, S.G., Lee, J.H., 2008. Modified transtrochanteric rotational osteotomy for femoral head osteonecrosis. Clin. Orthop. Relat. Res. 466, 1110–1116. https://doi.org/10.1007/s11999-008-0188-5.

Yoshida, H., Faust, A., Wilckens, J., Kitagawa, M., Fetto, J., Chao, E.Y.-S., 2006. Three-dimensional dynamic hip contact area and pressure distribution during activities of daily living. J. Biomech. 39, 1996–2004. https://doi.org/10.1016/j.jbiomech.2005.06.026.

Yushkevich, P.A., Piven, J., Hazlett, H.C., Smith, R.G., Ho, S., Gee, J.C., Gerig, G., 2006. User-guided 3D active contour segmentation of anatomical structures: significantly improved efficiency and reliability. Neuroimage 31, 1116–1128. https://doi.org/10.1016/j.neuroimage.2006.01.015.

Zhao, G., Yamamoto, T., Motomura, G., Iwasaki, K., Yamaguchi, R., Ikemura, S., Iwamoto, Y., 2013. Radiological outcome analyses of transtrochanteric posterior rotational osteotomy for osteonecrosis of the femoral head at a mean follow-up of 11 years. J. Orthop. Sci. 18, 277–283. https://doi.org/10.1007/s00776-012-0347-0.